Acta Geologica Polonica, Vol. 70 (2020), No. 1, pp. 97–106
DOI: 10.24425/agp.2019.126451

REVIEW PAPER

Chevkinite-group minerals in Poland

KRZYSZTOF NEJBERT[1], BOGUSŁAW BAGIŃSKI[1], JAKUB KOTOWSKI[1], PETRAS JOKUBAUSKAS[1], EDYTA JUREWICZ[1] and RAY MACDONALD[1, 2]

[1] *Faculty of Geology, University of Warsaw, PL-02-089 Warszawa, Poland.*
E-mails: knejbert@uw.edu.pl; b.baginski1@uw.edu.pl; jb.kotowski@gmail.com; klavishas@gmail.com; edyta.jurewicz@uw.edu.pl
[2] *Environment Centre, Lancaster University, Lancaster LA1 4YQ, United Kingdom.*
E-mail: r.macdonald@lancs.ac.uk

ABSTRACT:

Nejbert, K., Bagiński, B., Kotowski, J., Jokubauskas, P., Jurewicz, E. and Macdonald, R. 2020. Chevkinite-group minerals in Poland. *Acta Geologica Polonica*, **70** (1), 97–106. Warszawa.

The chevkinite group of minerals are REE,Ti-silicates increasingly recognized as widespread accessory phases in a wide range of igneous and metamorphic parageneses. Members of the group are here recorded from five localities in Poland: a two-pyroxene andesite from the Kłodzko-Złoty Stok intrusion, a trachyandesite intrusion north of the Pieniny Mountains, a rapakivi-type granite from the Krasnopol intrusion, an anorthosite from the Suwałki Anorthosite Massif, and nepheline syenite from the Ełk syenite massif. Specific members found are chevkinite-(Ce), perrierite-(Ce) and, potentially, the Al-dominant analogue of perrierite-(Ce). The case is made that chevkinite-group minerals will, through systematic investigation, be found in a wide range of Polish igneous and metamorphic rocks.

Key words: Chevkinite-group minerals; Chevkinite-(Ce); Perrierite-(Ce); Mineral chemistry; Petrological significance; Poland.

INTRODUCTION

The chevkinite-group of minerals (CGM) comprises twelve members (Table 1). The composition of the two most common members, chevkinite and perrierite, can be represented by the general formula $A_4BC_2D_2(Si_2O_7)_2O_8$, where A = REE, Ca, Sr, Th, B = Fe^{2+}, C = Fe^{2+}, Fe^{3+}, Mg, Al, Zr, Ti, and D = Ti. Chevkinite tends to have higher Fe and REE, and lower Ca, Sr, Ti and Zr contents than perrierite. Members can contain up to 50 wt.% REE_2O_3, especially the LREE, and can also contain substantial amounts of Th, Zr, Nb and Sc. In recent years it has become increasingly clear that the CGM are accessory phases in a very wide range of igneous and metamorphic rocks ranging from kimberlites through mafic to felsic types, granulites and gneisses, hydrothermal and pegmatitic rocks, skarns and ore deposits (Macdonald and Belkin 2002; Vlach and Gualda 2007; Carlier and Lorand 2008; Belkin *et al.* 2009; Macdonald *et al.* 2009, 2013, 2019; Bagiński and Macdonald 2013). Members of the group are known from hundreds of localities worldwide. In some rocks, for example Palaeogene granites in the Hebridean Igneous Province, UK, a CGM is the dominant REE-bearing phase (Macdonald *et al.* 2013). In such rocks, the CGM can play an important role in determining trace element behaviour during fractional crystallization and thus govern the potential of the system to build up large concentrations of these elements. Members of the group have also been used to determine the nature of hydrothermal fluids and in geochronological studies, as reviewed by Macdonald *et al.* (2019).

Any attempt to model the geochemical evolution of a rock suite on the basis of REE or other trace ele-

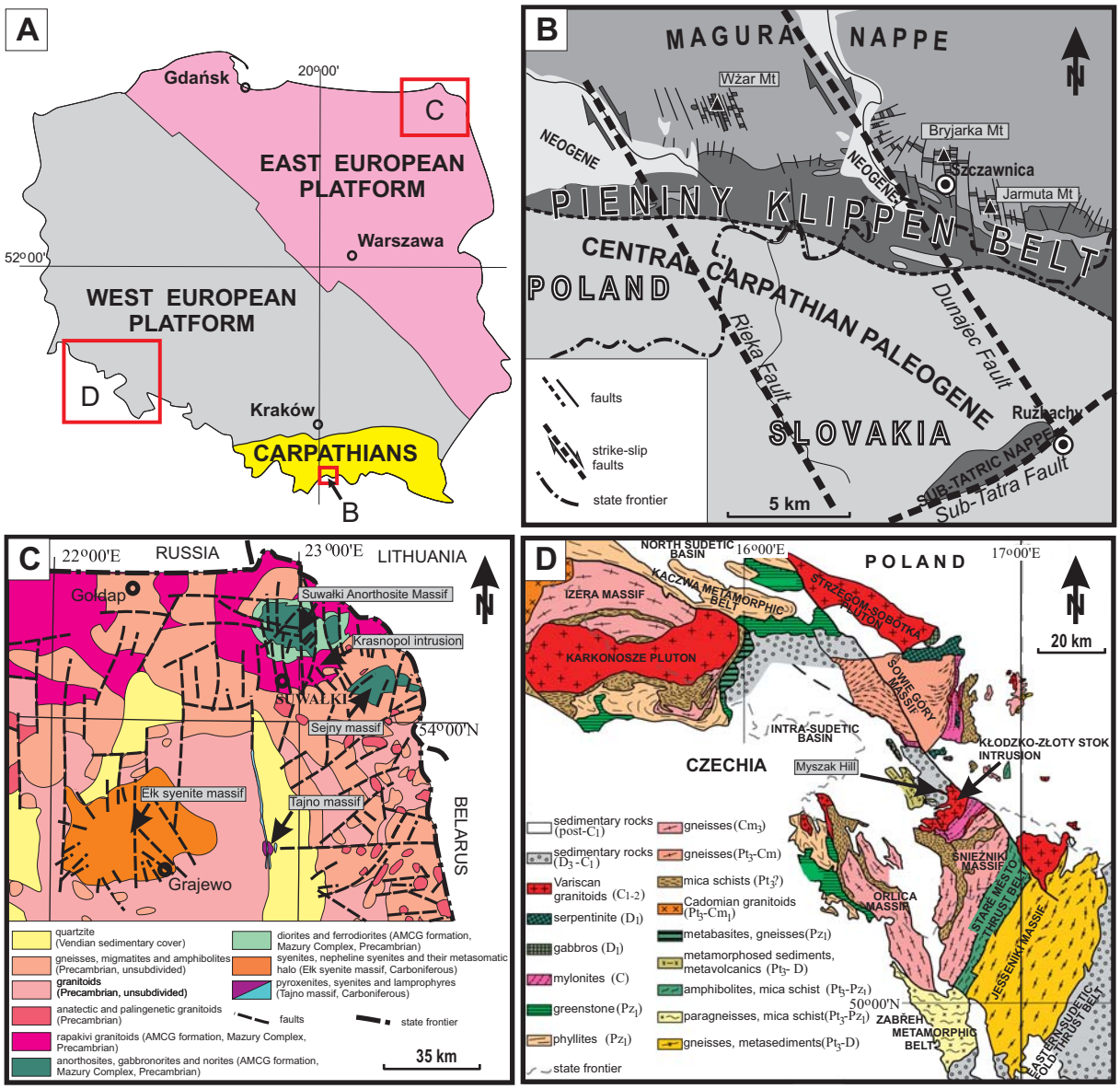

Text-fig. 1. Schematic geological maps illustrating localities in Poland where chevkinite occurrences have been documented. A – Main tectonic units in Poland (after Żelaźniewicz *et al.* 2011). B – Pieniny andesites (after Nejbert *et al.* 2012). C – Crystalline basement of the East European Platform (after Kubicki and Ryka 1982). D – Kłodzko-Złoty Stok granitic intrusion, Sudetes (after Mazur *et al.* 2006)

ments must take account of the possible contribution of CGM. Yet, as Bagiński and Macdonald (2013) have stressed, CGM have not generally been systematically sought for, or have been overlooked, in rocks in which they are potential phases. In Poland, for example, CGM have only been reported, in an abstract without documentation, in carbonatite veins from the Tajno massif, East European Platform (Pańczyk *et al.* 2015). We report here on the occurrence of CGM at five Polish localities (Text-fig. 1), where the host rocks have very different lithologies. We hope to encourage researchers to look for further occurrences.

SAMPLES AND ANALYTICAL METHODS

In our work, CGM are first sought using scanning electron microscopy, where their bright appearance makes them relatively easy to spot. Mineral compositions are then determined by electron microprobe

Mineral	Formula	Reference
Chevkinite subgroup		
Chevkinite-(Ce)	$(REE,Ca,Th)_4(Fe^{2+},Mg)(Fe^{2+},Ti,Fe^{3+})_2(Ti,Fe^{3+})_2(Si_2O_7)_2O_8$	Ito and Arem (1971)
Polyakovite-(Ce)	$(Ce,Ca)_4(Mg,Fe^{2+})(Cr^{3+},Fe^{3+})_2(Ti,Nb)_2(Si_2O_7)_2O_8$	Popov *et al.* (2001)
Maoniupingite-(Ce)	$(Ce,Ca)_4(Fe^{3+},Ti,Fe^{2+},\square)(Ti,Fe^{3+},Fe^{2+},Nb)_4(Si_2O_7)_2O_8$	Shen *et al.* (2005)
Dingdaohengite-(Ce)	$(Ce,La)_4Fe^{2+}(Ti,Fe^{2+},Mg,Fe^{3+})_2Ti_2(Si_2O_7)_2O_8$	Xu *et al.* (2008)
Christofschäferite-(Ce)	$(Ce,La,Ca)_4Mn(Ti,Fe^{3+})_3(Fe^{3+},Fe^{2+},Ti)(Si_2O_7)_2O_8$	Chukanov *et al.* (2012)
Delhuyarite-(Ce)	$Ce_4Mg(Fe^{3+},W)_3\square(Si_2O_7)_2O_6(OH)_2$	Holstam *et al.* (2017)
Perrierite subgroup		
Perrierite-(Ce)	$Ce_4MgFe^{3+}{}_2Ti_2(Si_2O_7)_2O_8$	Ito and Arem (1971)
Strontiochevkinite	$(Sr,La,Ce,Ca)_4Fe^{2+}(Ti,Zr)_2Ti_2(Si_2O_7)_2O_8$	Haggerty and Mariano (1983)
Rengeite	$Sr_4ZrTi_4(Si_2O_7)_2O_8$	Miyajima *et al.* (2001)
Matsubaraite	$Sr_4Ti_5(Si_2O_7)_2O_8$	Miyajima *et al.* (2002)
Hezuolinite	$(Sr,REE)_4Zr(Ti,Fe^{3+})_4(Si_2O_7)_2O_8$	Yang *et al.* (2012)
Perrierite-(La)	$(La,Ce,Ca)_4(Fe,Mn^{2+},Mg)Fe^{3+}{}_2(Ti,Fe^{3+})_2(Si_2O_7)_2O_8$	Chukanov *et al.* (2011)

Table 1. Members of the chevkinite-group of minerals accepted by the CNMNC-IMA

analysis at the Inter-Institute Analytical Complex at the IGMiP, Faculty of Geology, University of Warsaw, using a Cameca SX-100 microprobe equipped with four wavelength dispersive spectrometers. The accelerating voltage is 15 kV and the probe current is 20 nA. The standards and X-ray lines used are given in Suppl. Table 1 available only in online version. Standard counting times are 20 s on peak and 10 s on each of two background positions. The 'PAP' Φ(ρZ) program (Pouchou and Pichoir 1991) is used for corrections. Representative analyses are given in Table 2.

The most robust discriminant between chevkinite is the monoclinic β angle (~100º in chevkinite; ~113º in perrierite; Haggerty and Mariano 1983). However, to allow classifying the phases when no structural analysis is available, Macdonald *et al.* (2009) introduced an empirical discriminant based on a plot of (CaO+SrO) against FeO* (where FeO* is total Fe as Fe^{2+}). That classification scheme is followed here (Text-fig. 2).

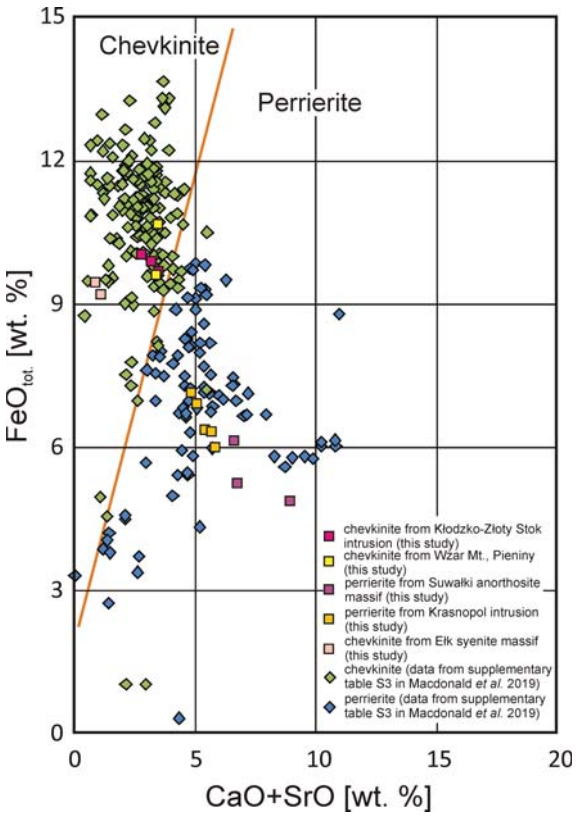

Text-fig. 2. (CaO+SrO) – FeO* discrimination plot, after Macdonald *et al.* (2009). Point analyses are those listed in Table 2 and marked on the relevant figures

KŁODZKO-ZŁOTY STOK INTRUSION, SUDETES, SOUTHWESTERN POLAND

The first recognition of a CGM in Poland was by Jokubauskas during his PhD studies (Jokubauskas 2017); the occurrence was in the Myszak dyke, a two-pyroxene basaltic andesite in the Variscan Kłodzko-Złoty Stok intrusion in the Sudetes (Text-fig. 1). The major minerals in the dyke are phenocrystic plagioclase (An_{30-90}), clinopyroxene and orthopyroxene, with relics of olivine, in a groundmass of alkali feldspar, plagioclase (An_{30}) and quartz. The accessory phases are apatite, zircon, ilmenite, spinel and chevkinite. The chevkinite is rare, occurring as fragmented, strongly oscillatory zoned crystals up to 100 μm long (Text-fig. 3). The dark areas are probably hydrothermally altered.

Compositional data for the unaltered phase are given in Table 2. The mineral is chevkinite-(Ce), with

Locality	Kłodzko-Złoty Stok intrusion			Mt Wżar, north of Pieniny Mts.		Suwałki Anorthosite Massif, Udryn area				Krasnopol intrusion, NE Poland				Ełk intrusion	
Rock type	basaltic andesite			andesite		gabbronorite				granitoid				syenite	
Analysis point	1	2	3	x1	x2	x1	x2	x3	x47	x50	x8	x9	x10	x33	x44
wt%															
P_2O_5	bd	0.06	bd	0.08	bd	bd	0.03	bd	–	–	–	–	–	bd	bd
SiO_2	19.26	19.35	19.17	22.64	19.53	21.35	20.48	24.02	20.19	20.37	20.45	20.40	20.48	18.29	18.68
TiO_2	17.70	17.81	17.24	16.03	17.28	19.43	18.18	16.43	17.58	18.23	17.15	17.06	16.88	16.68	17.54
ZrO_2	0.43	0.80	0.51	1.50	1.69	3.93	2.25	2.17	0.39	0.56	1.53	1.71	1.23	0.10	0.39
ThO_2	0.98	0.65	0.49	0.82	1.29	0.95	2.52	2.06	3.16	2.06	3.46	3.65	3.69	1.48	0.57
Nb_2O_5	0.23	0.14	0.22	1.10	1.28	0.18	0.14	bd	0.00	0.13	0.47	0.42	0.44	0.52	0.45
UO_2	0.20	0.16	0.12	0.09	bd	0.10	0.07	0.34	0.00	0.00	0.31	0.24	0.26	–	–
Ta_2O_5	bd	0.12	0.07	0.05	0.11	0.05	0.11	0.08	0.16	0.14	0.06	0.11	0.15	0.09	0.13
Al_2O_3	0.84	0.77	0.88	2.33	1.23	4.66	4.61	6.33	3.67	3.43	4.29	4.32	4.29	0.04	0.03
Sc_2O_3	0.26	0.18	0.17	–	–	0.49	0.45	0.37	0.27	0.31	0.10	0.12	0.12	0.02	–
Y_2O_3	1.33	1.52	1.34	0.46	0.43	0.37	0.62	0.33	0.20	0.28	0.98	1.02	1.01	0.13	0.181
La_2O_3	10.82	11.55	11.62	14.66	14.94	8.74	8.78	8.49	8.54	9.66	9.24	9.48	9.30	20.52	19.36
Ce_2O_3	20.79	20.67	21.73	19.73	19.87	16.01	17.08	15.35	17.01	19.01	17.47	17.04	17.43	22.30	22.34
Pr_2O_3	1.90	1.94	1.73	1.45	1.23	1.64	1.83	1.79	1.35	1.37	1.53	1.24	1.30	1.45	1.70
Nd_2O_3	6.26	5.86	6.66	3.50	3.86	4.68	5.57	5.29	5.90	5.68	5.07	5.32	5.19	3.54	4.02
Sm_2O_3	0.88	0.58	0.68	0.29	bd	0.16	0.58	0.43	0.52	0.31	0.54	0.75	0.78	–	0.41
Gd_2O_3	0.74	0.41	0.62	0.29	bd	0.33	0.49	0.27	0.24	0.40	0.45	0.46	0.35	–	0.41
MgO	0.35	0.32	0.37	0.38	0.37	0.45	0.65	0.54	0.81	0.90	0.74	0.70	0.75	0.09	0.11
CaO	3.19	3.47	2.78	3.38	3.48	8.96	6.63	6.75	4.86	5.10	5.84	5.67	5.43	0.84	1.05
MnO	0.11	0.09	0.13	0.24	0.41	0.08	0.08	0.13	0.00	0.00	0.09	0.12	0.11	2.29	2.18
FeO*	9.90	9.70	10.04	9.65	10.67	4.89	6.15	5.28	7.16	6.93	6.02	6.36	6.38	9.46	9.22
BaO	0.18	bd	bd	0.17	0.15	bd	0.07	0.31	–	–	–	–	–	bd	bd
Na_2O	bd	bd	bd	0.15	bd	bd	bd	bd	–	–	–	–	–	–	bd
Total	96.35	96.15	96.57	98.99	97.82	97.45	97.37	96.76	92.01	94.86	95.79	96.19	95.55	97.84	98.76
Σ REE_2O_3	42.72	42.53	44.38	40.38	40.33	31.93	34.33	31.95	33.56	36.44	34.30	34.28	34.34	47.81	48.23
Formulae on 22 oxygen basis															
Ca	0.724	0.783	0.633	0.713	0.768	1.810	0.239	1.356	1.078	1.106	1.251	1.212	1.169	0.196	0.242
Ba	0.015	0.000	0.000	0.013	0.012	0.000	18.207	0.005	0.000	0.000	0.000	0.000	0.000	0.000	0.000
Na	0.000	0.000	0.000	0.057	0.000	0.000	0.000	0.000	–	–	–	–	–	–	0.000
La	0.845	0.898	0.911	1.065	1.135	0.608	0.109	0.587	0.653	0.721	0.681	0.698	0.689	1.658	1.533
Ce	1.612	1.595	1.691	1.423	1.499	1.105	0.211	1.054	1.291	1.409	1.278	1.246	1.282	1.788	1.756
Pr	0.147	0.149	0.134	0.104	0.092	0.113	0.022	0.122	0.102	0.101	0.111	0.090	0.095	0.115	0.133
Nd	0.473	0.441	0.505	0.246	0.284	0.315	0.067	0.354	0.437	0.410	0.362	0.379	0.372	0.277	0.308
Sm	0.064	0.042	0.050	0.020	0.000	0.010	0.007	0.028	0.037	0.022	0.037	0.052	0.054	–	0.030
Gd	0.052	0.029	0.044	0.019	0.000	0.021	0.005	0.017	0.016	0.027	0.030	0.030	0.024	–	0.029
Y	0.150	0.170	0.152	0.048	0.047	0.037	0.011	0.033	0.022	0.030	0.104	0.108	0.108	0.015	0.021
Th	0.047	0.031	0.024	0.037	0.060	0.041	0.019	0.088	0.149	0.095	0.157	0.166	0.169	0.074	0.028
U	0.009	0.008	0.006	0.004	0.000	0.004	0.001	0.014	0.000	0.000	0.014	0.011	0.011	–	–
Sum A	4.138	4.146	4.148	3.749	3.898	4.063	18.898	3.658	3.786	3.922	4.026	3.992	3.973	4.124	4.079
Fe^{2+}	1.000	1.000	1.000	1.000	1.000	0.771	1.000	0.828	1.000	1.000	1.000	1.000	1.000	1.000	1.000
Mn	0.000	0.000	0.000	0.000	0.000	0.013	0.000	0.021	0.000	0.000	0.000	0.000	0.000	0.000	0.000
Mg	0.000	0.000	0.000	0.000	0.000	0.126	0.000	0.151	0.000	0.000	0.000	0.000	0.000	0.000	0.000
Sum B	1.000	1.000	1.000	1.000	1.000	0.910	1.000	0.999	1.000	1.000	1.000	1.000	1.000	1.000	1.000
Fe^{2+}	0.753	0.709	0.784	0.589	0.838	0.000	0.004	0.000	0.241	0.172	0.006	0.062	0.076	0.733	0.654
Mn	0.020	0.016	0.023	0.040	0.072	0.000	0.002	0.000	0.000	0.000	0.015	0.021	0.019	0.425	0.397
Mg	0.110	0.100	0.117	0.112	0.114	0.000	0.033	0.000	0.251	0.271	0.221	0.209	0.223	0.028	0.036
Nb	0.022	0.013	0.021	0.098	0.119	0.015	0.002	0.000	0.000	0.012	0.042	0.038	0.040	0.052	0.044

Locality	Kłodzko-Złoty Stok intrusion			Mt Wżar, north of Pieniny Mts.		Suwałki Anorthosite Massif, Udryn area				Krasnopol intrusion, NE Poland				Ełk intrusion	
Rock type	basaltic andesite			andesite		gabbronorite				granitoid				syenite	
Analysis point	1	2	3	x1	x2	x1	x2	x3	x47	x50	x8	x9	x10	x33	x44
Ta	0.000	0.007	0.004	0.003	0.006	0.003	0.001	0.004	0.009	0.008	0.003	0.006	0.008	0.005	0.008
Zr	0.044	0.082	0.053	0.144	0.170	0.361	0.037	0.198	0.040	0.055	0.149	0.166	0.121	0.010	0.040
Al	0.210	0.191	0.220	0.541	0.299	1.035	0.183	1.399	0.897	0.817	1.011	1.017	1.015	0.010	0.007
Ti	0.818	0.822	0.755	0.374	0.677	0.754	0.669	0.315	0.739	0.775	0.578	0.561	0.563	0.748	0.831
Sum C	1.978	1.942	1.978	1.900	2.294	2.169	0.931	1.916	2.177	2.110	2.026	2.081	2.066	2.011	2.017
D (= Ti)	2.000	2.000	2.000	2.000	2.000	2.000	2.000	2.000	2.000	2.000	2.000	2.000	2.000	2.000	2.000
Si	4.078	4.077	4.073	4.458	4.023	4.024	0.689	4.503	4.184	4.123	4.087	4.073	4.116	4.006	4.009
P	0.000	0.011	0.000	0.013	0.000	0.000	0.001	0.000	0.000	0.000	0.000	0.000	0.000	0.000	0.000
Sum T	4.078	4.088	4.073	4.472	4.023	4.024	0.690	4.503	4.184	4.123	4.087	4.073	4.116	4.006	4.009
Cations	13.19	13.18	13.20	13.12	13.22	13.17	23.52	13.08	13.15	13.15	13.14	13.15	13.16	13.14	13.11

Table 2. Compositions of chevkinite-group minerals from Polish localities. Analysis points as marked on relevant figures. FeO*, all Fe as Fe^{2+}; bd indicates below detection limit; – indicates not determined

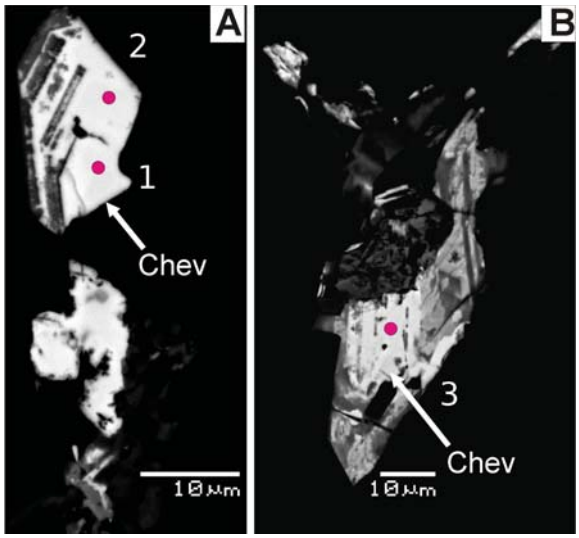

Text-fig. 3. BSE images of complexly zoned, hydrothermally altered and fractured chevkinite-(Ce) from the Kłodzko-Złoty Stok intrusion. The point analyses marked in pink are given in Table 2. Abbreviations: Chev – chevkinite

Ti dominant in the C site. There are minor amounts of Al (≤0.21 a.p.f.u.), Mg (≤0.11 a.p.f.u.) and Zr (≤0.06 a.p.f.u.). The average formula is:

$$[(Ce_{1.63}La_{0.88}Ca_{0.71}Nd_{0.47}Y_{0.16}Pr_{0.14})_{3.99}$$
$$Fe^{2+}(Ti_{0.79}Fe^{2+}{}_{0.75}Al_{0.21}Mg_{0.11}Zr_{0.06})_{1.92}$$
$$Ti_2(Si2_{.03}O_7)_2O_8].$$

MT WŻAR, NORTH OF PIENINY MTS., OUTER CARPATHIANS, SOUTHERN POLAND

Chevkinite-group minerals have been documented during petrological studies of small-volume intrusions of andesites occurring in the Outer Carpathians in Poland (near the Pieniny Mts.) and in similar rocks occurring in Moravia in the Uherski Brod region (Nejbert *et al.* 2012, 2013; Macdonald *et al.* 2018). Larger amounts of CGM were found in alkaline andesite in Moravia (Nejbert *et al.* 2013; Macdonald *et al.* 2018), while in Poland CGM occur in small amounts in the form of microcrystals in the matrix of a hornblende trachyandesite from Wżar Mt. (Text-fig. 1).

Text-fig. 4 is a BSE image of chevkinite in a Miocene trachyandesite intrusion at Wżar Mt. near the Pieniny Mountains. The phase is very rare: so far, only one crystal has been identified, occurring as a lath interstitial to plagioclase in a trachyandesite containing large (from 0.5 to 4 cm in diameter) clinopyroxene, hornblende and plagioclase phenocrysts. The

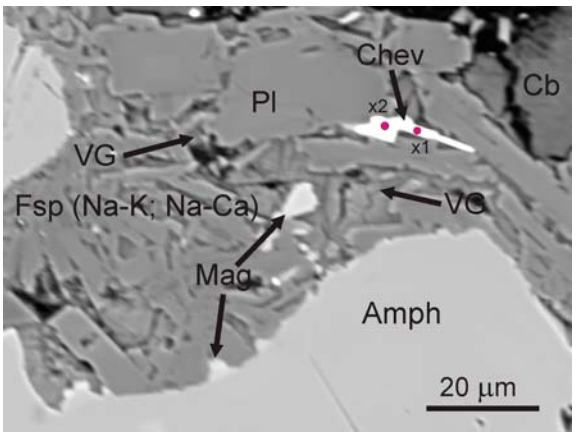

Text-fig. 4. Chevkinite-(Ce) in (trachy)andesite intrusion, Wżar Mt., in the vicinity of Pieniny Mts. The point analyses marked in pink are given in Table 2. Abbreviations: Amph – amphibole, Cb – carbonate mineral (dolomite), Chev – chevkinite-(Ce), Fsp Na-K – Na-K feldspar, Fsp Na-Ca – sodic plagioclase, Mag – magnetite, Pl – plagioclase, VG – volcanic glass

rock matrix is dominated by small sodic plagioclases, Na-K feldspars, quartz, Ti-magnetite and ilmenite, with accessory apatite and zircon. Two point analyses are presented in Table 2, showing that the phase is chevkinite-(Ce). Analysis 2 has a slight deficiency in the A site (3.7 a.p.f.u.), suggesting some secondary hydration, and excess Si (4.4 a.p.f.u.) related to beam contamination. In analysis 1, Fe is dominant in the C site where there are moderate amounts of Al (0.30 a.p.f.u.), Zr (0.17 a.p.f.u.) and Mg (0.11 a.p.f.u.). The formula is:

$$[(Ce_{1.50}La_{1.14}Ca_{0.77}Nd_{0.28}Pr_{0.09}Th_{0.06}Y_{0.05})_{3.9}$$
$$Fe^{2+}(Fe^{2+}_{0.84}Ti_{0.68}Al_{0.30}Zr_{0.17}Nb_{0.12}Mg_{0.11})_{2.2}$$
$$Ti_2(Si_{2.01}O_7)_2O_8].$$

SUWAŁKI ANORTHOSITE MASSIF, MAZURY COMPLEX, NORTEASTERN POLAND

The tectonic setting of the Mesoproterozoic magmatism of the Mazury Complex, NE Poland, is thought to be an E-W trending belt of post-collisional provenance (Text-fig. 1). Several intrusions of anorogenic character, including rapakivi-type granites and anorthosite-norite massifs (Suwałki, Sejny, Kętrzyn) have been identified (Kubicki and Ryka 1982). The anorthosite-norite rocks of Suwałki were part of the oldest magmatic episode in the complex and have been dated (Re-Os on Ti-magnetite and sulphides) at 1599±37 Ma and 1569±94 (Stein *et al.* 1998; Morgan *et al.* 2000; Wiszniewska 2002).

Chevkinite-group minerals are present in both the Krasnopol granite intrusion (see below) and Suwałki Anorthosite Massif. Text-fig. 5A, B are BSE images of a CGM in gabbronorite from the Udryn-4 borehole in the Suwałki intrusion. The small (~10 μm) anhedral grain in Text-fig. 5B is associated with ilmenite, baddeleyite and pyrrhotite. In Text-fig. 5C, it forms a prism enclosed in alkali feldspar and a slightly rounded grain associated with ilmenite. Also present is an unidentified Ti-Fe-Zr phase.

The high Al_2O_3 contents of the Suwałki phase (4.61–6.33 wt.%; Table 2) result in Al being the dominant cation in the C site (1.03–1.37 a.p.f.u.), which potentially makes it the Al-dominant analogue of perrierite-(Ce). This, therefore, is a particularly interesting locality: such highly aluminous CGM have previously been recorded only from high-grade metamorphic rocks of Antarctica (Harley 1994; Hokada 2007; Belkin *et al.* 2009). The high Al is very probably related to its occurrence in anorthosite.

The textural position of the CGM indicates that their growth was related to K-feldspar exsolution

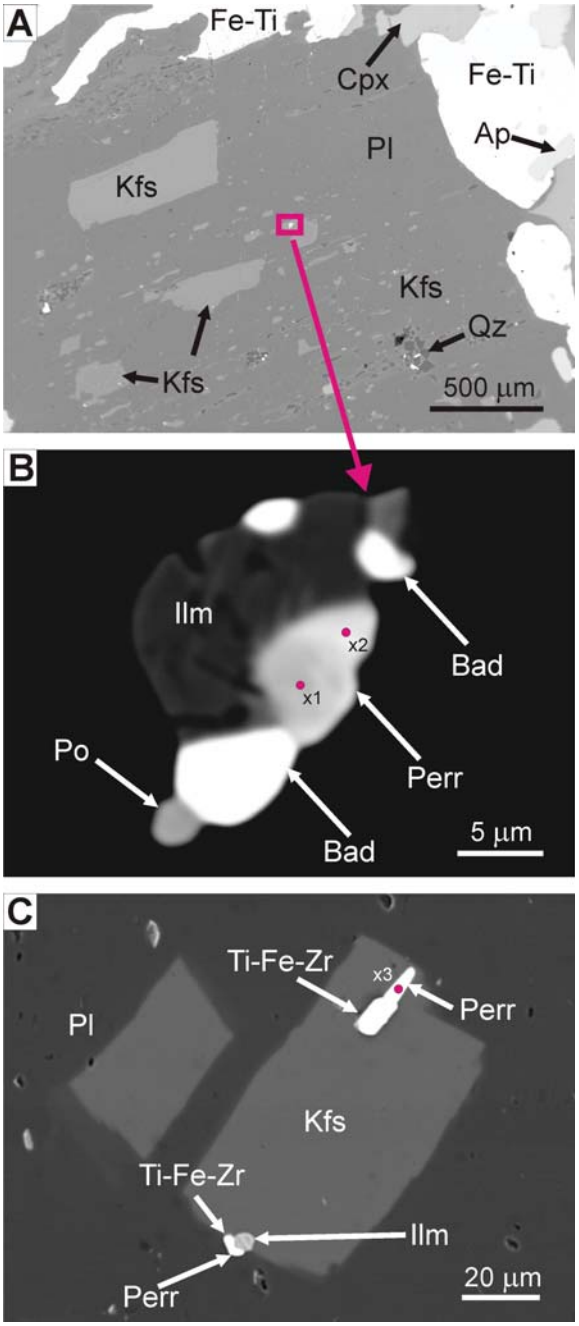

Text-fig. 5. BSE images of perrierite-(Ce) from gabbronorite of the Suwałki Anorthosite Massif. A-B – Anhedral perrierite-(Ce) and associated ilmenite, baddeleyite and pyrrhotite attached to alkali feldspar in gabbronorite. C – Perrierite-(Ce) prism enclosed in alkali feldspar, gabbronorite. The phase marked Ti-Fe-Zr is unidentified. The rounded grain at the bottom marked Perr (perrierite) has been identified from its EDS spectrum. The point analyses marked in pink are given in Table 2. Abbreviations: Ap – apatite, Bad – baddeleyite, Cpx – clinopyroxene, Fe-Ti – magnetite and/or ilmenite, Ilm – ilmenite, Kfs – K feldspar, Perr – perrierite-(Ce), Pl – plagioclase, Po – pyrrhotite, Qz – quartz, Ti-Fe-Zr – unidentified mineral with Fe, Ti, and Zr in the structure

from plagioclase (Text-fig. 5A–C), occurring just after the solidification of anorthosite melts, probably at depths of 10 to 20 km (Ashval 1993). Thus, recrystallization of feldspars took place under P-T conditions typical of the granulite facies. These conditions are commonly recorded in contact aureoles around anorthosite massifs (Maijer 1981; Åreback and Andersson 2002; Westphal *et al.* 2003). Similar P-T conditions were confirmed during an experimental study of crystallization of magmatic jotunite from the Rogaland Anorthosite Complex (Vander Auwera and Longhi 1994).

KRASNOPOL INTRUSION, MAZURY COMPLEX, NORTHEASTERN POLAND

The Krasnopol granitoid intrusion is located between the Suwałki Anorthosite Massif and the Sejny Massif, in whose central part there are small magmatic intrusions of anorthosite and ferrodiorite/jotunite (Text-fig. 1). The Krasnopol monzodiorite/granodiorite has a U-Pb zircon age close to 1525±4 Ma (Dörr *et al.* 2002). Magmatic rocks of the Sejny Massif also represent an early magmatic episode in the Mazury Complex, and the monzodiorites (jotunites) have been dated from 1549±5 Ma to 1519+17/-12 Ma by the U-Pb method on single crystals (Gawęda *et al.* 2005).

The magmatic rocks of the Krasnopol intrusion, made available by Krasopol PIG-6 drilling, are similar to rocks from the Pawłówka PIG-1, Filipów IG-1 and Bartoszyce IG-1 boreholes (Bagiński *et al.* 2001; Dörr *et al.* 2002). Petrographically and geochemically, they are a diverse set of granitoids with phyric texture whose systematic nomenclature varies from monzodiorite to granodiorite; however, many of the samples are quartz monzodiorites and quartz monzonites (Bagiński *et al.* 2001; Dörr *et al.* 2002). The SiO_2 contents of the Krasnopol rocks vary from 51.6 to 61.1 wt.%. They are metaluminous, with the geochemical characteristics of A-type granitoids (Bagiński *et al.* 2001; Dörr *et al.* 2002).

Ongoing studies by KN and JK of rocks from the Krasnopol 6 borehole, from the central part of the Krasnopol granitoid intrusion, are showing that they contain abundant CGM. Crystals are up to 400 mm in size and vary in form from ragged anhedral grains (Text-fig. 6A) to subhedral plates (Text-fig. 6B). A notable feature is that crystals are commonly hydrothermally altered; on BSE images high-Z cores are mantled by patchy grey altered zones (Text-fig. 6). The low analytical totals (92.02–96.19 wt.%) and the small deficiencies in the A site (3.79–4.02 a.p.f.u.) almost certainly indicate that the crystals have been secondarily hydrated (Table 2). The CGM grains from the Krasnopol granitic intrusion are perrierite-(Ce) (Text-fig. 2) and like the Suwalki CGM are unusual in being the Al-dominant analogue of the mineral.

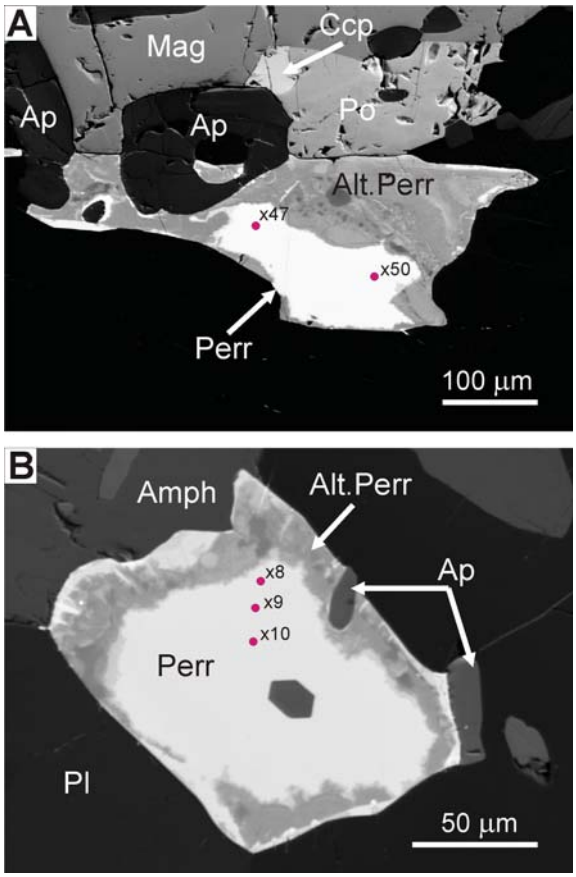

Text-fig. 6. BSE images of CGM in the Krasnopol granitic intrusion. A – Ragged, elongated plate with a bright (high Z) core of perrierite-(Ce), with a patchily zoned mantle of altered perrierite. B – Subhedral plate of perrierite-(Ce) with patchily zoned rim of altered material. The point analyses marked in pink are given in Table 2. Abbreviations: Amph – amphibole, Alt. Perr – altered perrierite, Ap – apatite, Ccp – chalcopyrite, Mag – magnetite, Perr – perrierite-(Ce), Pl – plagioclase, Po – pyrrhotite

EŁK SYENITE MASSIF, CRYSTALLINE BASEMENT OF EAST EUROPEAN PLATFORM, NORTHEASTERN POLAND

Chevkinite-group minerals are rather common in syenites of the Carboniferous Ełk syenite massif (ESM) (Krzemińska *et al.* 2006; Demaiffe *et al.*

2013), which occurs in the crystalline basement of NE Poland and is buried under a thick (600–800 m) Meso-Cenozoic cover (Ryka 1994). The analyzed samples were collected from core material and are representative of the central part of the Ełk syenite massif (Krystkiewicz and Ryka 1994). The crystals in Text-fig. 7 occur in a medium-grained nepheline syenite with dispersed intergrowths of aegirine. In Text-fig. 7A chevkinite-(Ce) forms an arcuate aggregate, totalling ca. 320 μm in length, elongated along the boundaries between alkali feldspar crystals. One grain in Text-fig. 7B is prismatic, partly resorbed and some 105×45 μm in size. It includes a rounded, dark grey crystal, so far unidentified. The other grain is ragged, platy, and 130×105 μm in size. The platy grain is subtly zoned from brighter (higher Z) to lower areas of brightness. It is overgrown by allanite.

Representative compositions are given in Table 2. The mineral is chevkinite-(Ce), with Ti dominant in the C site. The main substituents are Mn, Nb, Th and Zr. The MnO contents are relatively high for chevkinite: in their compilation of 164 analyses of chevkinite, Macdonald *et al.* (2019) found the average abundances to be 0.54±0.67 wt.% MnO. The average formula can be written as:

$$[(Ce_{1.81}La_{1.38}Nd_{0.33}Ca_{0.29}Th_{0.07})_{3.9}$$
$$Fe^{2+}(Ti_{0.84}Fe^{2+}_{0.66}Mn_{0.41}Nb_{0.05}Zr_{0.05})_{2.0}$$
$$Ti_2(Si_{2.0}O_7)_2O_8].$$

The detailed relationships between textural type, composition and zonation merit our ongoing detailed study of the Ełk CGM.

CONCLUDING REMARKS

We stress that these reports are not a result of a systematic search for CGM. Rather, being aware of their possible existence in various suites that we were studying, the CGM were identified quickly. This gives us confidence that CGM are present in a wide range of Polish rocks, including further examples from the Variscan granitoids, the Carboniferous intrusions of Mazury, and the AMGC suites of Mazury. A CGM has recently been found in the Žermanice sill in the Czech segment of the teschenitic association of southern Poland-Czech Republic (Matýsek *et al.* 2018), and must surely also be present in the Polish segment. Other potential occurrences are in the granulite facies rocks of the East European Craton, and the volcanic rocks associated with the Variscan granitoid intrusions in SW Poland. As this work has shown, CGM are not restricted to alkaline igneous rocks, as commonly supposed.

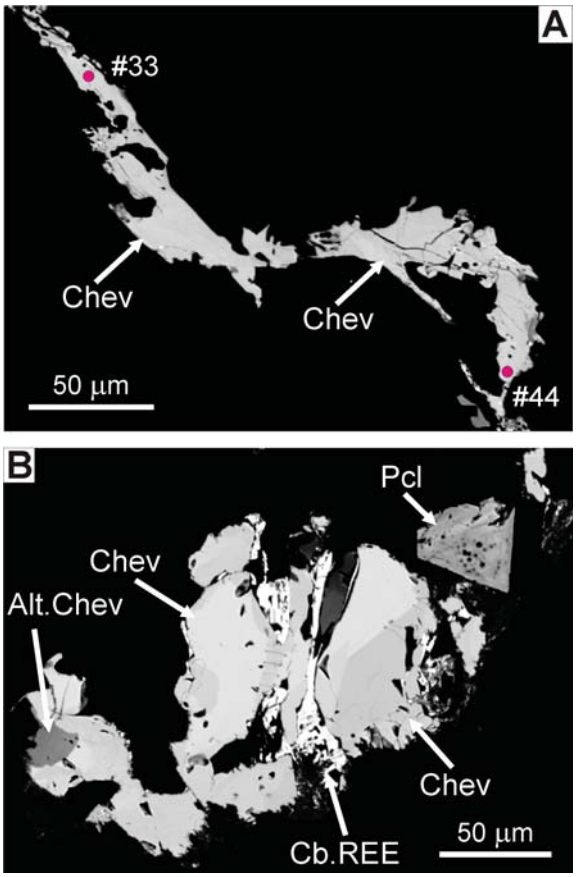

Text-fig. 7. BSE images of CGM from the Ełk massif. A – Aggregate of chevkinite-(Ce) grains along the boundaries between alkali feldspar crystals. Point analyses marked in pink are given in Table 2. B – Ragged, partly resorbed, platy and prismatic crystals of chevkinite-(Ce). Abbreviations: Alt. Chev – altered chevkinite, Cb. REE – REE carbonates, Chev – chevkinite, Pcl – pyrochlore

Acknowledgements

We thank Ms Lidia Jeżak and Dr. Beata Marciniak-Maliszewska for help in performing EPMA analyses. Special thanks are given to Prof. Igor Broska and Prof. Andrzej Muszyński for their critical and constructive remarks on the manuscript.

REFERENCES

Åreback, H. and Andersson, U.B. 2002. Granulite-facies contact metamorphism around the Hakefjorden Norite-Anorthosite Complex, SW Sweden. *Norsk Geologisk Tidsskrift*, **82**, 29–44.

Ashval, L.D. 1993. Anorthosites, 422 p. Springer Verlag; Berlin.

Bagiński, B., Duchesne, J.C., Vander Auwera, J., Martin, H.

and Wiszniewska, J. 2001. Petrology and geochemistry of rapakivi-type granites from the crystalline basement of NE Poland. *Geological Quarterly*, **45**, 33–52.

Bagiński, B. and Macdonald, R. 2013. The chevkinite group: underestimated accessory phases from a wide range of parageneses. *Mineralogia*, **44**, 99–114.

Belkin, H.E., Macdonald, R. and Grew, E.S. 2009. Chevkinite-group minerals from granulite-facies metamorphic rocks and associated pegmatites of East Africa and South India. *Mineralogical Magazine*, **73**, 149–164.

Carlier, G. and Lorand, J.-P. 2008. Zr-rich accessory minerals (titanite, perrierite, zirconolite, baddeleyite) record strong oxidation associated with magma mixing in the south Peruvian potassic province. *Lithos*, **104**, 54–70.

Chukanov, N.V., Aksenov, S.M., Rastsvetaeva, R.K., Belakovskiy D.I., Göttlicher, J., Britvin, S.N. and Möckel S. 2012. Christofschäferite-(Ce), Ce,La,Ca)$_4$Mn^{2+}(Ti,Fe^{3+})$_3$(Fe^{3+},Fe^{2+},Ti)(Si$_2$O$_7$)$_2$O$_8$ – a new chevkinite-group mineral from the Eifel area, Germany. *New Data on Minerals*, **47**, 33–42.

Chukanov, N.V., Blass, G., Pekov, I.V., Belakovskiy, D.I., Van, K.V., Rastsvetaeva, R.K. and Aksenov, S.M. 2011. Perrierite-(La), (La,Ce,Ca)$_4$Fe^{2+}(Ti,Fe)$_4$(Si$_2$O$_7$)$_2$O$_8$, a new mineral species from the Eifel volcanic area, Germany. *Zapiski Rossiiskogo Mineralogicheskogo Obshchestva*, **140**, 34–44. [In Russian]

Demaiffe, D., Wiszniewska, J., Krzemińska, E., Williams, I.S., Stein, H., Brassinnes, S., Ohnenstetter, D. and Deloule, E.A. 2013. Hidden alkaline and carbonatite province of Early Carboniferous age in northeast Poland: zircon U-Pb and pyrrhotite Re-Os geochronology. *The Journal of Geology*, **121**, 91–104.

Dörr, W., Belka, Z., Marheine, D., Schastok, J., Valverde-Vaquero, P. and Wiszniewska, J. 2002. U-Pb and Ar-Ar geochronology of anorogenic granite magmatism of the Mazury complex NE Poland. *Precambrian Research*, **119**, 101–120.

Dubińska, E., Bylina, P., Kozłowski, A., Dörr, W., Nejbert, K., Schastok, J. and Kulicki, C. 2004. U-Pb dating of serpentinization: hydrothermal zircon from a metasomatic rodingite shell (Sudetic ophiolite, SW Poland). *Chemical Geology*, **203**, 183–203.

Gawęda, A., Wiszniewska, J. and Dörr, W. 2005. Polystage mafic plutonism within AMCG Mazury Complex – The Sejny IG-1 borehole, NE Poland. *Polskie Towarzystwo Mineralogiczne – Prace Specjalne*, **26**, 36–39.

Haggerty, S.E. and Mariano, A.N. 1983. Strontian-loparite and strontio-chevkinite: Two new minerals in rheomorphic fenites from the Paraná Basin carbonatites, South America. *Contributions to Mineralogy and Petrology*, **84**, 365–381.

Harley, S.L. 1994. Mg-Al yttrian zirconolite in a partially melted sapphirine granulite, Vestfold Hills, East Antarctica. *Mineralogical Magazine*, **58**, 259–269.

Hokada, T. 2007. Perrierite in sapphirine-quartz gneiss: geochemical and geochronological features and implications for accessory-phase paragenesis of UHT metamorphism. *Journal of Mineralogical and Petrological Sciences*, **102**, 44–49.

Holtstam, D., Bindi, L., Hålenius, U. and Andersson, U.B. 2017. Delhuyarite-(Ce) Ce$_4$Mg(Fe$^{3+}_2$W)□(Si$_2$O$_7$)$_2$O$_6$(OH)$_2$ a new mineral of the chevkinite group, from the Nya Bastnäs Fe-Cu-REE deposit, Sweden. *European Journal of Mineralogy*, **29**, 897–905.

Ito, J. and Arem, J.E. 1971. Chevkinite and perrierite; synthesis, crystal growth, and polymorphism. *American Mineralogist*, **56**, 307–319.

Jarosewich, E. and Boatner, L. 1991. Rare-earth element reference samples for electron microprobe analysis. *Geostandards and Geoanalytical Research*, **15**, 397–399.

Jokubauskas, P. 2017. The magma system of the Kłodzko-Złoty Stok intrusion, 154 p. Unpublished PhD thesis, University of Warsaw.

Krystkiewicz, E. and Ryka, W. 1994. Petrography of the Ełk Syenite Massif. *Prace Państwowego Instytutu Geologicznego*, **144**, 19–48.

Krzemińska, E., Wiszniewska, J. and Williams, I.S. 2006. Early Carboniferous age of the cratonic intrusions in the crystalline basement of NE Poland. *Przegląd Geologiczny*, **54**, 1093–1098.

Kubicki, S. and Ryka, W. 1982. Geological atlas of crystalline basement in Polish part of the east-European platform. Wydawnictwa Geologiczne: Warszawa. [In Polish]

Macdonald, R. and Belkin, H.E. 2002. Compositional variation in minerals of the chevkinite group. *Mineralogical Magazine*, **66**, 1075–1098.

Macdonald, R., Belkin, H.E., Wall, F. and Bagiński, B. 2009. Compositional variation in the chevkinite group: new data from igneous and metamorphic rocks. *Mineralogical Magazine*, **73**, 777–796.

Macdonald, R., Bagiński, B., Dzierżanowski, P., Fettes, D.J. and Upton, B.G.J. 2013. Chevkinite-group minerals in UK Palaeogene granites: underestimated REE-bearing accessory phases. *The Canadian Mineralogist*, **51**, 333–347.

Macdonald, R., Bagiński, B., Belkin, H.E. and Stachowicz, M. 2019. Composition, paragenesis, and alteration of the chevkinite group of minerals. *American Mineralogist*, **104**, 348–369.

Macdonald, R., Nejbert, K., Jurewicz, E. and Bagiński, B. 2018. Ti-Zr-Nb-bearing accessory minerals in high-K trachyandesitic rocks from the Western Outer Carpathians, Moravia, Czech. *European Journal of Mineralogy*, **30**, 135–147.

Maijer, C., Andriessen, P.A.M., Hebeda, E.H., Jansen, J.B.H. and Verschure, R.H. 1981. Osumilite, an approximately 970 Ma old high-temperature index mineral of the granulite-facies metamorphism in Rogaland, SW Norway. *Geologie en Mijnbouw*, **60**, 267–272.

Matýsek, D., Brásek, J., Skupien, P. and Thomson, S.N. 2018. The Žermanice sill: new insights into the mineralogy, petrology, age, and origin of the teschenite association rocks

in the Western Carpathians, Czech Republic. *International Journal of Earth Sciences*, **107**, 2553–2574.

Mazur, S., Aleksandrowski, P. and Szczepański, J. 2010. Outline structure and tectonic evolution of the Variscan Sudetes. *Przegląd Geologiczny*, **58**, 133–145. [In Polish with English abstract]

Miyajima, H., Matsubara, S., Miyawaki, R., Yokoyama, K. and Hirokawa, K. 2001. Rengeite, $Sr_4ZrTi_4Si_4O_{22}$, a new mineral, the Sr-Zr analogue of perrierite from the Itoigawa-Ohmi district, Niigata Prefecture, central Japan. *Mineralogical Magazine*, **65**, 111–120.

Miyajima, H., Miyawaki, R. and Ito, K. 2002. Matsubaraite, $Sr_4Ti_5(Si_2O_7)_2O_8$, a new mineral, the SrTi analog of perrierite in jadeitite from the Itoigawa-Ohmi District, Niigata Prefecture. Japan. *European Journal of Mineralogy*, **14**, 1119–1128.

Morgan, J.W., Stein, H.J., Hannah, J.L., Markey, R.J. and Wiszniewska, J. 2000. Re-Os study of Fe-Ti-V oxide and Fe-Cu-Ni sulfide deposits, Suwałki Anorthosite Massif, northeast Poland. *Mineralium Deposita*, **35**, 391–401.

Nejbert, K., Jurewicz, E. and Macdonald, R. 2012. High-K magmatism in the Western Outer Carpathians: magma-genesis in the transitional zone between the European Plate and Carpathian-Pannonian region. *Lithos*, **146-147**, 34–47.

Nejbert, K., Macdonald, R. and Jurewicz, E. 2013. Mineral chemistry of chevkinite group minerals from andesitic of the Western Outer Carparthians. In: Büchner, J., Rapprich, V. and Tietz, O. (Eds), Basalt 2013 Cenozoic Magmatism in Central Europe. 24th to 25th April 2013, Görlitz/Germany. Abstracts & Excursion Guides, pp. 104–105.

Pańczyk, M., Bazarnik, J., Zieliński, G., Giro, L., Nawrocki, J. and Krzemiński, L. 2015. REE bearing minerals in carbonatite veins from the Tajno massif (East European Platform, NE Poland). *Mineralogia – Special Papers*, **44**, 80–81.

Popov, V.A., Pautov, L.A., Sokolova, E., Hawthorne, F.C., McCammon, C. and Bazhenova, L. 2001. Polyakovite-(Ce), $(REE,Ca)_4(Mg,Fe^{2+})(Cr^{3+},Fe^{3+})_2Si_8O_{22}$, a new metamict mineral species from the Ilmen mountains, Southern Urals, Russia: Mineral description and crystal chemistry. *Canadian Mineralogist*, **39**, 1095–1104.

Pouchou, J.L. and Pichoir, J.F. 1991. Quantitative analysis of homogeneous or stratified microvolumes applying the model 'PAP'. In: Heinrich, K.F.J. and Newbury, H. (Eds), Electron Probe Quantitation. pp. 31–76. Plenum Press; New York.

Ryka, W. (Ed.) 1994. Geology of the Ełk syenite massif (northeastern Poland). *Prace Państwowego Instytutu Geologicznego*, **144**, 1–125.

Shen, G., Yang, G. and Xu, J. 2005. Maoniupingite-Ce: A new rare earth mineral from the Maoniuping rare-earth deposit in Mianning, Sichuan. *Sedimentary Geology and Tethyan Geology*, **25**, 210–216. [In Chinese with English abstract]

Stein, H.J., Morgan, J.W., Markey, R.J. and Wiszniewska, J. 1998. A Re/Os study of the Suwalki anorthosite massif, Northeast Poland. EUROBRIDGE 1998. *Geophysical Journal*, **20**, 111–113.

Vander Auwera, J. and Longhi, J. 1994. Experimental study of a jotunite (hypersthene monzodiorite): constraints on the parent magma composition and crystallization conditions (P, T, fO_2) of the Bjerkreim-Sokndal layered intrusion (Norway). *Contributions to Mineralogy and Petrology*, **118**, 60–78.

Vlach, S.R.F. and Gualda, G.A.R. 2007. Allanite and chevkinite in A-type granites and syenites of the Graciosa Province, southern Brazil. *Lithos*, **97**, 98–121.

Westphal, M., Schumacher, J.C. and Boschert, S. 2003. High-temperature metamorphism and the role of magmatic heat sources at the Rogaland Anorthosite Complex in southwestern Norway. *Journal of Petrology*, **44**, 1145–1162.

Wiszniewska, J. 2002. Age and the genesis of Fe-Ti-V ores and related rocks in the Suwałki Anorthosite Massif (northeastern Poland). *Biuletyn Państwowego Instytutu Geologicznego*, **401**, 1–96. [In Polish]

Xu, J., Yang, G., Li, G., Wu, Z. and Shen, G. 2008. Dingdaohengite-(Ce) from the Bayan Obo REE-Nb-Fe Mine, China: Both a true polymorph of perrierite-(Ce) and a titanic analog at the C1 site of chevkinite subgroup. 2008. *American Mineralogist*, **93**, 740–744.

Yang, Z., Giester, G., Ding, K. and Tillmans, E. 2012. Hezuolinite, $(Sr,REE)_4Zr(Ti,Fe^{3+},Fe^{2+})_2Ti_2O_8(Si_2O_7)_2$, a new mineral species of the chevkinite group from Saima alkaline complex in Liaoning Province, NE China. *European Journal of Mineralogy*, **24**, 189–196.

Żelaźniewicz, A., Aleksandrowski, P., Buła, Z., Karnkowski, P., Konon, A., Oszczypko, N., Ślączka, A., Żaba, J. and Żytko, K. 2011. Tectonic subdivision of Poland, 60 p. Komitet Nauk Geologicznych PAN; Wrocław. [In Polish]

Manuscript submitted: 1st May 2019
Revised version accepted: 30th September 2019

Supplementary-table 1. Analytical details of EPMA (CAMECA SX100)

Element	Line	Crystal	Standard	Detection limit (wt.%)
Al	Ka	TAP	orthoclase	0.008
Ba	La	LiF	baryte	0.114
Ca	Ka	PET	$CaSiO_3$	0.008
Ce	Ka	PET	CeP_5O_{14}	0.053
Dy	Lb	LiF	REE1*	0.312
Eu	Lb	LiF	REE2*	0.263
Fe	Ka	LiF	hematite	0.034
Gd	Lb	LiF	GdP_5O_{14}	0.126
Hf	Ma	TAP	Hf-SPI	0.033
La	La	PET	LaB6	0.052
Mg	Ka	TAP	diopside	0.006
Mn	Ka	LiF	rhodonite	0.036
Na	Ka	TAP	albite	0.012
Nb	La	PET	Nb metal	0.054
Nd	Lb	LiF	NdP_5O_{14}	0.121
P	Ka	PET	Apatite Jap2	0.014
Pr	Lb	LiF	PrP_5O_{14}	0.119
Sc	Ka	PET	Sc metal	0.01
Si	Ka	TAP	$CaSiO_3$	0.006
Sm	Lb	LiF	SmP_5O_{14}	0.115
Sr	La	TAP	$SrTiO_3$	0.027
Ta	Ma	TAP	Ta metal	0.036
Tb	La	LiF	REE4*	0.144
Th	Ma	PET	ThO_2 synthetic	0.086
Ti	Ka	PET	rutile	0.016
U	Mb	PET	vorlanite ($CaUO_4$)	0.077
Y	La	TAP	$Y_3Al_5O_{12}$	0.028
Yb	La	LiF	REE3*	0.136
Zr	La	PET	Zircon ED2**	0.051

* the acronyms REE1-4 refer to glasses containing REE (for details see Jarosewich and Boatner 1991); ** zircon standard from the Gogołów -Jordanów serpentinite massif (for details see Dubińska *et al.* 2004).